



**HAL**  
open science

## Macrophage polarization in vitro and in vivo modified by contact with fragmented chitosan hydrogel

Ysander von Boxberg, Sylvia Soares, Camille Giraudon, Laurent David, Maud Viallon, Alexandra Montembault, Fatiha Nothias

### ► To cite this version:

Ysander von Boxberg, Sylvia Soares, Camille Giraudon, Laurent David, Maud Viallon, et al.. Macrophage polarization in vitro and in vivo modified by contact with fragmented chitosan hydrogel. Journal of Biomedical Materials Research Part A, 2022, 110 (4), pp.773-787. 10.1002/jbm.a.37326 . hal-03414668

**HAL Id: hal-03414668**

**<https://hal.sorbonne-universite.fr/hal-03414668>**

Submitted on 4 Nov 2021

**HAL** is a multi-disciplinary open access archive for the deposit and dissemination of scientific research documents, whether they are published or not. The documents may come from teaching and research institutions in France or abroad, or from public or private research centers.

L'archive ouverte pluridisciplinaire **HAL**, est destinée au dépôt et à la diffusion de documents scientifiques de niveau recherche, publiés ou non, émanant des établissements d'enseignement et de recherche français ou étrangers, des laboratoires publics ou privés.

# Macrophage polarization *in vitro* and *in vivo* modified by contact with fragmented chitosan hydrogel

***Running title: Chitosan hydrogel and inflammation***

Ysander von Boxberg<sup>1,2,3\*</sup>, Sylvia Soares<sup>1,2,3</sup>, Camille Giraudon<sup>1,2,3</sup>, Laurent David<sup>4,5</sup>, Maud Viallon<sup>4,5</sup>, Alexandra Montembault<sup>4,5</sup>, Fatiha Nothias<sup>1,2,3\*</sup>

<sup>1</sup> Sorbonne Universités, UPMC Paris 06, UM 119, Institut de Biologie Paris Seine IBPS, F-75005 Paris, France

<sup>2</sup> CNRS UMR 8246, Neurosciences Paris Seine NPS, F-75005 Paris, France

<sup>3</sup> INSERM U 1130, Neurosciences Paris Seine NPS, F-75005 Paris, France

<sup>4</sup> Université de Lyon, Université Claude Bernard Lyon-1, F-69622 Villeurbanne, France

<sup>5</sup> CNRS UMR 5223 Ingénierie des Matériaux Polymères IMP, F-69622 Villeurbanne, France

\* Corresponding authors

ysander.von\_boxberg@upmc.fr; fatiha.nothias@upmc.fr

## **Acknowledgments:**

The present work was supported by SATT-Lutech (Société d'Accélération du Transfert de Technologies - Lutech), Paris.

## ABSTRACT

We have previously shown that implantation of a fragmented chitosan hydrogel suspension (chitosan-FPHS) into a traumatic spinal cord lesion in adult rats led to significant axon regrowth and functional recovery, which was associated to a modulation of inflammation. Using an *in vitro* culture system, we show here that polarization of bone marrow-derived macrophages is indeed modified by direct contact with chitosan-FPHS. Reducing the degree of acetylation (DA), and raising the concentration of chitosan (Cp, from 1.5% to 3%), favors macrophage polarization towards anti-inflammatory subtypes. These latter also migrate and adhere efficiently on low, but not high DA chitosan-FPHS, both *in vitro* and *in vivo*, while inflammatory macrophages rarely invade a chitosan-FPHS implant *in vivo*, no matter the DA. Our *in vitro* model setup should prove a valuable tool for screening diverse biomaterial formulations and combinations thereof for their inflammatory potential prior to implantation *in vivo*.

### **Keywords**

*chitosan hydrogel; acetylation degree; inflammation; bone marrow macrophages; cell culture; spinal cord injury*

### **Abbreviations**

FPHS: fragmented physical hydrogel suspension; DA: degree of acetylation; Cp: chitosan concentration in hydrogel; MΦ: macrophage(s); SCI: spinal cord injury; TCP: tissue culture plastic; PLL: poly-L-lysine; COS: chito-oligosaccharides; PEG: poly-ethylene glycol

## 1. INTRODUCTION

Inflammation is an important step in the process of wound healing, necessary to clean up damaged tissue and pave the way for its reconstruction. Wounded tissue is thus rapidly infiltrated by leukocytes and other lymphocytes, soon followed by circulating inflammatory macrophages (often termed "M1" macrophages) that in turn, are then gradually replaced by different subtypes of "alternatively activated", non-inflammatory macrophages ("M2"). These latter participate actively in the reconstitution of the lesioned tissue by favoring extracellular matrix deposition, cell proliferation, neoangiogenesis, and finally scar resorption ("resolution" phase). Macrophages (M $\Phi$  hereafter) are very dynamic cells, capable of rapidly switching phenotype depending on environmental factors<sup>1</sup>.

In case of traumatic injury to the central nervous system, in particular the spinal cord, the above sequence of the diverse M $\Phi$  phenotypes assuring the process from cleaning up to tissue reconstruction is desynchronized<sup>2</sup>. After a spinal cord injury (SCI), inflammation is almost immediately triggered by activation of tissue-resident microglia, rapidly exacerbated by the release of cytotoxic/inflammatory factors like excess glutamate and free radicals (ROS [reactive oxygen species]), NO [nitric oxide]) from damaged cells, and invasion of circulating monocytes/M $\Phi$  following breakage of the blood-spinal cord barrier<sup>3</sup>. The majority of the latter being of the M1 type (the classic first step of an acute immune response) they will release mostly inflammatory cytokines and thus attract even more M1 M $\Phi$  to the lesion site. Not least due to degeneration of damaged axons and the associated release of myelin debris, inflammation then spreads from the initial impact site towards neighboring segments, whereas "beneficial" M2 M $\Phi$ , initially also present, rapidly disappear<sup>4</sup>. Indeed, inflammation of the injured spinal tissue may persist almost indefinitely, further aggravating the initial damage. Therefore, new concepts for spinal cord injury (SCI) therapies will likely include immune modulatory approaches, targeting a timed balance between inflammatory (M1), and inflammation-resolving, tissue-remodeling (M2) M $\Phi$ <sup>5-9</sup>.

We have previously shown<sup>10</sup> that implantation into a rat spinal cord lesion site (dorsal hemisection lesion) of a dense suspension of chitosan hydrogel particles (termed chitosan-FPHS, fragmented physical hydrogel suspension) is by itself able to initiate neural tissue reconstruction, revascularization, and axon regrowth while at the same

time reducing glial scarring, accompanied by significant functional recovery. Chitosan is generated by deacetylation of chitin, a copolymer of  $\beta$ -(1-4)-linked D-glucosamine and N-acetyl-D-glucosamine units, present for example in the exoskeleton of crustaceans and in cell walls of fungi. Chitosan has proved to be a highly biocompatible (non-toxic), biodegradable natural polymer with interesting antibacterial and antifungal properties. Prepared in various forms, such as nanoparticles<sup>11</sup>, electrospun fibers (in a polymer mixture with collagen and thermoplastic polyurethane<sup>12</sup>), or as physical hydrogels, it has already been employed in a number of biomedical applications, e.g. as wound dressing<sup>13</sup>, drug delivery vehicle<sup>14</sup>, and most interestingly, in various tissue-engineering strategies<sup>15-17</sup>. Chitosan has already been used for experimental SCI treatment, but usually as support structure for trophic factor delivery, or cell therapy<sup>18,19</sup>; for review<sup>20</sup>. The particular chitosan formulation we used for implantation into the rat SCI site<sup>10</sup> was prepared from squid pen, and had a weight-averaged molar mass ( $M_w$ ) of  $\sim 550,000$  g/mol, a degree of acetylation (DA) of 4% (i.e. highly deacetylated chitosan, equivalent to a deacetylation degree [DD] of 96%), a chitosan concentration (w/w) in the hydrogel (Cp) of 2.5%, and above all, was fragmented with particle sizes mainly ranging from 20 to 100 $\mu$ m (i.e. about the size of cells). The highly beneficial effect of implantation of this chitosan-FPHS was associated with a modulation of the inflammatory response around the lesion site, allowing for a long-term presence of M2, and reduced numbers of M1 M $\Phi$ , as visualized both by immunohistochemistry, and Western blotting for specific M $\Phi$  marker proteins. Here, we wanted to address the question whether this immunomodulatory effect was directly related to the physico-chemical properties of chitosan-FPHS interacting with M $\Phi$ , or rather secondary to the many other changes elicited by its implantation, such as extracellular matrix deposition, invasion of diverse cell types, reduced astroglial activation, and reconstitution of a functional blood-spinal cord barrier. The *in vitro* approaches presented in this study should be valuable for testing the reaction of immune cells to chitosan-FPHS and derivatives with variable parameters, as well as other biomaterials, before a potential application as bio-scaffold *in vivo*.

## 2. MATERIALS AND METHODS

### 2.1 Animals

All experiments were carried out in compliance with 2010/63/UE European directive and French decree 2013-118, and approved by the Institutional Animal Care and Ethics Committee at Sorbonne University (#1514.01).

Adult female Wistar rats (ca. 230-250g) to be used for spinal cord injury were bought from Janvier, France. Macrophages were produced from femur bones of C57bl6 mice housed in our animal facilities, and which after removal of femur bones were usually exploited for other cell or tissue culture experiments at the same time.

### 2.2 Chitosan substrate preparation

Chitosan-FPHS was generated as described previously<sup>10,16</sup>. Briefly, squid pen chitosan powder (Mahtani, India) was further purified by dissolving in acetic acid, filtering, and re-precipitation with ammonia solution, followed by freeze drying after extensive washing in deionized water. Degree of acetylation (DA) was determined by <sup>1</sup>H-NMR spectroscopy, and when needed, reacylation was performed with stoichiometric addition of acetic anhydride to hydro-alcoholic chitosan solutions<sup>21</sup>. Purified chitosan powder (reacylated or not) was then solubilized in dilute acetic acid at a given concentration (w/w), and a hydrogel disc formed by exposing the solution contained in a 35mm Petri dish over a source of ammonia vapors (generated with a 1M aqueous ammonia solution) for at least 3h, again followed by extensive washing until obtaining a neutral pH. This hydrogel was then fragmented in a large volume (10:1) of deionized water using an Ultra-Turrax (IKA) blender to generate a suspension with a medium fragment size of ~20µm, which was passed through a 100µm pore size mesh for further homogenization of particle size (see also Fig. 1a), and finally autoclaved (20 min at 121°C, +1 bar).

To create a cell culture substrate, the suspension was concentrated by brief centrifugation (1 min/2000g, minifuge), discarding the supernatant, and after resuspension in a small volume of the original dilute hydrogel particle suspension, the

slurry was evenly applied to the bottom of 12-well culture plates (Nunclon, Thermo Scientific), and left to adhere to the tissue culture plastic (TCP), or to glass coverslips under a sterile hood until the excess water from the suspension had evaporated (see Fig. 1B). Glass coverslips (18 mm  $\varnothing$ ) were pre-treated with 50  $\mu\text{g}/\text{mL}$  poly-L-lysine (PLL) in sterile  $\text{H}_2\text{O}$  for 3 h, rinsed in water and dried before applying the chitosan-FPHS slurry. Before seeding monocytes on the resulting layer of chitosan-FPHS with its slightly granular appearance, the latter was covered with culture medium for at least 2 h.

Different concentrations of chitosan within the hydrogel (Cp), and different acetylation degrees (DA) were used in this study. Since generation of a stable culture substrate necessitated evaporation of excess water from the suspension, we also determined the final concentration the cells were actually exposed to, by weighing the mass  $m_1$  of culture plates covered with a stable layer of chitosan-FPHS (as used for cell seeding), and the mass  $m_2$  of the same plates after complete drying (5 days at  $37^\circ\text{C}$ ). Final chitosan concentration was then calculated as  $0.9 * m_2/m_1$ , assuming that the dried hydrogel still contains about 10% water.

### **2.3 Preparation of mouse bone marrow monocytes/macrophages**

Young (<3 months) C57BL/6 mice (Janvier, France) were anesthetized with isoflurane and killed by cervical dislocation. Femur bones (with hip and knee joints intact), dissected under semi-sterile conditions, were freed of any attached tissue, briefly dipped in 70% ethanol to dehydrate any remaining muscle tissue, then rinsed in D-PBS without  $\text{Ca}^{++}/\text{Mg}^{++}$  (Gibco) before cutting off the two extremities. The bone marrow was extracted into ice-cold PBS by pushing it out of the bone cavity with a stream of PBS from a syringe equipped with a 25G needle. It was then centrifuged (800 rpm, 5 min; Heraeus table top centrifuge), and resuspended in macrophage complete medium. Complete macrophage culture medium was composed of 20% homemade L929-conditioned medium, 10% FCS, 1% penicillin/streptomycin (Sigma) in DMEM (Gibco), sterile-filtered before use. L929-conditioned medium was prepared by growing this fibroblast cell line in DMEM or DMEM-F12 medium supplemented with 10% FCS and penicillin/streptomycin in T75 culture flasks until near-confluence. The culture supernatant was harvested, and stored at  $-80^\circ\text{C}$ . This protocol is adapted from<sup>22</sup>.

Bone marrow cells were seeded in 15 mL of macrophage complete medium at a density of  $\sim 4 \times 10^5$  cells per 10 cm  $\varnothing$  culture plate (bacterial grade plastic), and grown for 7 days, adding 10 mL of fresh medium after 4 days. Monocytes were harvested by incubation for about 15 min with 5mM EGTA solution in PBS pH 7.4 under shaking, centrifuged and resuspended in complete culture medium.

## 2.4 Macrophage cultures

For Western blotting experiments, monocytes were seeded in 12-well culture plates (Nunclon, Thermo Scientific), coated or not with a chitosan-FPHS layer, at a density of  $\sim 60,000$  cells in 1 mL of culture medium per well, and incubated at 37°C/5% CO<sub>2</sub>. For immunocytochemistry, cells were seeded in 12-well plates onto 18 mm diameter coverslips that had been; PLL-treated coverslips were then covered, or not, with chitosan-FPHS slurry (about 150 $\mu$ L) as described above. Cell density was about 60,000 to 80,000 cells per well (in 1mL culture medium). For M $\Phi$  polarization, recombinant murine IFN- $\gamma$  (interferon-gamma, final concentration 25 ng/mL, Peprotech, Rocky Hill, NJ, USA) was added after 6-12h of culture to wells destined for M1 polarization, followed 6 h later by addition of LPS (lipopolysaccharide, 100 ng/mL, Sigma) to the same wells, or recombinant murine IL-4 (interleukine-4, 15 ng/mL, Peprotech) to wells destined for M2 polarization. M1/M2 M $\Phi$  polarization was monitored (*cf.* Fig. 1C-D) using an inverted phase contrast microscope (Nikon TS100), and cells were generally cultured for  $\sim 48$  h after addition of polarizing factors, unless otherwise indicated. In some conditions, 1 mg/mL of commercially available COS (chito-oligosaccharides) were added to the cultures together with the polarizing factors. These specific COS had a  $M_w \leq 1500$  g/mol and a DA  $\sim 8,5\%$  (MedChemExpress, Monmouth Junction, NJ, USA).

For insert cultures, preparation of the different types is schematized in Fig. 3. M $\Phi$  were either seeded on the insert membrane (3.0  $\mu$ m pores; "ThinCerts", Greiner bio-one) without addition of chitosan to the culture system (*cf.* Fig. 3a), or they were seeded on the bottom of the culture well, and a dense chitosan particle suspension in culture medium was added within the insert (Fig. 3b), or a chitosan particle film was generated on the bottom of the well as described above, and M $\Phi$  were seeded on the insert membrane touching the chitosan layer (Fig. 3c). For trans-pore migration (transwell)

assays, transparent ThinCerts with 8.0 $\mu$ m pore diameter were used. M $\Phi$  were seeded onto the insert membrane as illustrated in Fig. 3c, after verifying that the membrane was well in contact with the re-wetted chitosan layer, applied in this case onto PLL-pretreated 18 mm coverslips.

## 2.5 Protein lysis, Western blotting and antibodies

M $\Phi$  cultures in 12-well plates, both on tissue culture plastic and on chitosan granular layers, were lysed directly using ice-cold Laemmli lysis buffer (about 30 $\mu$ L per well) and a cell scraper. Lysates were stored on ice until the treatment of all wells was completed. Tubes with lysates were then briefly centrifuged, heated to 95°C for 3 min, vortexed, re-centrifuged, and again brought to 95°C for one more minute, before being stored at -20°C until further use.

SDS gel electrophoresis on a microscale (100  $\mu$ m thick slab gels) and transfer onto nitrocellulose membrane (Protran 0.45 $\mu$ m, GE healthcare) were done as described in <sup>23</sup>. Before loading onto the gel, chitosan-containing samples had to be centrifuged for at least 5 min at 14000g to separate lysate from hydrogel particles (some "smearing" of bands seen in figures of Western blots may be due to remaining chitosan particles in the samples). After transfer, membranes were blocked for 1h in 5% fat-free milk powder in PBS, before incubation with primary antibodies diluted in 5% milk powder/PBS/0.1% Tween-20 overnight. The following antibodies were used: mouse monoclonal anti- $\beta$ -actin (Santa Cruz, "C4"; 1:500), mouse monoclonal anti-mouse iNOS (BectonDickinson-Transduction Lab; 1:1500); goat anti-mannose receptor CD206 (Thermofisher; 1:500); rabbit anti-arginase-1 (Thermofisher; 1:1000). Secondary antibodies were alkaline phosphatase-coupled (Jackson ImmunoResearch), and reactive protein bands revealed using homemade NBT/BCIP (Roth Sochiel) reagent in TRIS-Mg<sup>2+</sup> buffer pH 9.5. Note that before incubation with primary antibodies membranes were usually cut in two, the lower part was reacted with actin, or arginase-1 plus actin antibodies, the upper part with iNOS, or CD206 antibodies, respectively. In the figures, actin bands (43 kDa) are always shown at the bottom, although the molecular weight of arginase-1 is actually

lower (35 kDa; approximate molecular weights of iNOS and CD206 are 130 kDa, and about 175 kDa, respectively).

## 2.6 Statistical analysis

Western blots were dried and mounted on cardboard, scanned (in black & white; Epson Perfection V500), and staining intensity of protein bands of interest evaluated using ImageStudioLite software (Li-Cor Biotechnology), using the  $\beta$ -actin band intensity corresponding to each sample for normalization. Care was taken to avoid saturated blacks during scanning, as they are not accepted by the software. For each experiment, intensity values of a marker protein band were arbitrarily set to 1 (i.e. 100%), and the relative intensities of the other bands expressed as fractions of the corresponding reference band value. For statistical analysis, at least 3 independent experiments (from cell culture to Western blotting) were exploited; sample sizes 'n' are indicated in the corresponding figure legends. Marker protein levels were compared between different experimental conditions using either a Student's t-test (Fig. 2), or a one-way ANOVA with Tukey's post-hoc multiple comparisons test run in GraphPad Prism software (Figs. 4 and 7), with statistical significance marked by asterisks corresponding to: \*  $p \leq 0.05$ , \*\*  $p \leq 0.01$ , \*\*\*  $p \leq 0.001$ , \*\*\*\*  $p \leq 0.0001$ .

## 2.7 Immunocyto- and histochemistry

Cultures on glass coverslips were fixed by addition of 1 ml/well of prewarmed, phosphate buffered 8% paraformaldehyde (PFA) solution for 20 min, then rinsed thoroughly in PBS. Cells were permeabilized by incubation in 0.3% Triton-X100/PBS for 15 min, and non-specific binding sites blocked in 10% BSA/PBS (bovine serum albumin, Euromedex) for 1h before further treatment. To visualize cell shape, F-actin was stained using phalloidin-AF488 (1/300, 2h; ThermoFisher), mitotic cells were labeled with rabbit- $\alpha$ -Ki67 antibody (1/100, over night; Novus Biologicals), and cell nuclei with DAPI (5 min, ThermoFisher), all diluted in 5% BSA/PBS with 0.05% Triton-X100. Coverslips were finally mounted onto microscope slides using Mowiol mounting medium, and photographed on a Leica DMRB fluorescence microscope (Leica, Wetzlar, Germany). Cell or nuclei counting was done on microphotographs using the particle count function of Fiji application (ImageJ v. 2.0).

For immunolabeling of spinal cord sections, they were first permeabilized by incubation in 0.3% Triton X-100/PBS during 5 min at room temperature, and blocked for 1 h in 10% BSA (bovine serum albumin)/PBS, before incubation overnight at room temperature with primary antibodies diluted in 5% BSA/PBS. To localize macrophages, primary antibodies used were rabbit anti-CD86 (Abcam, 1:1000), goat anti-CD206 (Thermofisher, 1:200). After washing in PBS (3 x 5 min), sections were reacted for at least 1h with appropriate Alexa-488 (1:1000), or Alexa-555 (1:1000)-coupled secondary antibodies, and DAPI for nuclear staining. After careful rinsing, sections were finally unfolded, dried and mounted in Mowiol. Microphotographs were taken on a Zeiss apotome-equipped inverted fluorescence microscope (Axiovert M200).

## 2.8 Surgical procedures

Animals were housed in the animal facilities of the IBPS institute. Before and after surgical interventions, food and water were available *ad libitum*. Before surgery, animals were subcutaneously injected with buprenorphine (Axience® 0.3 mg/mL) to reduce postoperative pain. Animals were placed on a heating surgical pad to maintain body temperature at 37°C, and were anesthetized *via* a surgical mask with isoflurane using 3% for induction, and 2% for anesthesia maintenance (TEM SEGA, France). The thoracic area was shaved, povidone-iodine (Vétoquinol, France) and alcohol applied to the skin, and eyes protected with a lubricant (Humigel, Virbac, France). Dorsal hemisection and chitosan-FPHS implantation were performed as described<sup>10</sup>. Briefly, after laminectomy at T8-T9 the *dura* was incised longitudinally, and a dorsal over-hemisection performed with surgical micro-scissors, followed by passing an ophthalmic micro-scalpel three times through the lesion for complete ablation of fiber pathways down to below the central canal. Except for lesioned control animals, a dense slurry of chitosan-FPHS (ca. 5 µL), obtained by brief centrifugation of the dilute suspension, was then injected into the injury site. Muscles were sutured, the skin closed using surgical staples, and Povidone-iodine applied to the wound. To prevent urinary infections, rats received subcutaneous injections of enrofloxacin (Baytril 10%, Bayer) once a day during the first week post-lesion. Until restoration of normal micturition, bladders were manually emptied daily, and the health state of operated rats monitored by regular weighing and visual inspection of the surgical wound.

Operated animals were subjected to open-field testing (BBB locomotor scale) the first day post-lesion (d+1), and then once a week. To ensure that lesion severity was comparable between animals, only animals with a BBB score of "0" at d+1 were evaluated. For immunohistochemical analysis of lesioned spinal cords 2 weeks post-injury, animals were deeply anesthetized by intraperitoneal injection of pentobarbital (Euthasol® 400mg/mL, 150 mg/Kg), and transcardially perfused first with saline at 37°C, then with 4% paraformaldehyde (PFA) in 0.1 M phosphate buffer. Spinal cords were dissected, post-fixed in PFA, cryoprotected by 30% sucrose, embedded in O.C.T. compound (Tissue-Tek), and stored at -80 °C. Horizontal sections (40 µm) were prepared on a cryostat (Leica CM3050 S), and mounted on glass slides (Superfrost® Plus).

### 3. RESULTS

#### 3.1 Chitosan-FPHS substrate modifies macrophage polarization

For the present study, we first prepared fragmented physical hydrogel suspensions of chitosan (chitosan-FPHS; **Fig 1a**, left) of the same type as those that we previously implanted *in vivo* into traumatic central nervous system injury sites in the rat<sup>10</sup>. Here, chitosan-FPHS was used as culture substrate for primary mouse bone marrow monocyte-derived M $\Phi$ , polarized into either M1 or M2 subtypes by addition of IFN $\gamma$ /LPS, or IL-4, respectively. To create the substrate, a concentrated chitosan particle suspension was evenly dispersed and left to adhere on the bottom of cell culture wells, yielding a film-like layer with rough surface, sticking firmly to the tissue culture plastic (**Fig 1a**, right). Monocytes were allowed to adhere to the substrate for at least 6 hours (usually overnight) before the addition of polarizing factors, and cultures were usually maintained for 48h after polarizing factor addition. **Fig 1b** illustrates the typical morphologies displayed by M1 (rounded, "fried egg shape") and M2 (elongated, irregularly shaped) polarized M $\Phi$  cultured on a "neutral" substrate (tissue culture plastic or glass) vs. chitosan-FPHS, on which they maintain a similar overall appearance, although the size of especially M1 M $\Phi$  is reduced. Western blotting of protein samples extracted from these cultures showed that fragmented chitosan hydrogel substrate had a direct impact on M $\Phi$  polarization (**Fig 2**): thus, in comparison to M $\Phi$  grown on tissue culture plastic (TCP, controls), on chitosan substrate the expression of M1 marker protein (iNOS) was reduced in IFN- $\gamma$ /LPS stimulated M $\Phi$ , while that of typical M2 marker proteins (Arginase-1, as well as Mannose Receptor [CD206]), was enhanced in IL-4 stimulated cells. Both changes are highly significant. Stimulation of Arg-1 expression by M $\Phi$  growing on chitosan-FPHS substrate was more pronounced than that of CD206, suggesting that the biomaterial differently impacts the expression of these two M2 marker proteins (note that in the spinal cord lesion site, Arg-1 expressing M $\Phi$  are rather short-lived, in contrast to CD206 expressing M $\Phi$  that may persist for weeks, particularly after chitosan-FPHS implantation<sup>10,24</sup>; see also **Fig. S2**).

### 3.2 Polarizing effect of chitosan-FPHS is contact-dependent

To determine whether direct contact between M $\Phi$  and chitosan-FPHS substrate is necessary for the re-polarizing effect to occur, different types of insert cultures were prepared: M $\Phi$  were thus grown on the porous membrane of culture inserts placed in wells the bottom of which was covered or not with chitosan-FPHS (**Fig. 3a,b**), or on the bottom of a culture well equipped with an insert filled with a chitosan particle slurry above the membrane (**Fig. 3c**). The pore diameter of 3 $\mu$ m allowed for exchange of solutes, but not crossing of cells. Western blotting showed that the presence or not of chitosan-FPHS in these cultures had no impact on M1 or M2 marker protein expression, indicating that direct contact to the chitosan hydrogel substrate is a prerequisite for the polarizing effect on M $\Phi$  described in Fig 2. This assay also indicates that the negative impact of the biomaterial on M1 M $\Phi$  polarization (Fig 2) should not be due to a potential absorption of polarizing factors by the hydrogel particles, since M1 marker protein expression is not affected by the presence of chitosan-FPHS in the culture medium (Fig. 3c).

### 3.3 Influence of chitosan concentration and acetylation degree

Next, we sought to determine how variations in the formulation of the hydrogel (concentration Cp, and degree of acetylation DA) would influence the effect on M $\Phi$  polarization. While the initial concentration (Cp) of chitosan-FPHS used *in vivo*<sup>10</sup> had been 2.5% chitosan/water (w/w), here we tested concentrations ranging from 1.5% to 3% Cp (note that due to the method of substrate creation by eliminating excess water from the hydrogel suspension, the actual Cp values seen by the cells were higher than those indicated in Fig 4 (*cf.* Materials and Methods; thus, an initial Cp of 1.5% becomes approximately 2.8%, 2% becomes 3.5%, 2.5% becomes 4.1%, and 3% becomes 4.7%). The initial DA of our chitosan-FPHS had been 4%, and we now employed chitosan formulations with a DA varying between 2% and 15%. As shown in **Fig. 4**, expression of M1 marker protein iNOS was significantly lower on chitosan-FPHS than on a neutral substrate (TCP). Increasing the concentration of chitosan in the hydrogel (Cp) resulted in a clear tendency of iNOS levels to decrease even further, although differences between individual Cp values were not significant. Varying the DA from 2% to 15%

resulted in the opposite phenomenon: iNOS expression significantly increased with increasing DA, reaching almost the same level as on TCP substrate for 11% and 15% DA chitosan-FPHS. Unfortunately, we were unable to test the reaction of M $\Phi$  to chitosan-FPHS with higher DA than 15%, as such hydrogels become too soft, and seem to "trap" lysed proteins that can no longer be extracted for SDS-electrophoresis. For M2 M $\Phi$ , arginase-1 levels were significantly higher on chitosan-FPHS than on TCP substrate, and there was a tendency of arginase-1 expression to increase with rising Cp (albeit not significant between individual Cp values). In contrast, changes in the DA had little influence on arginase-1 levels. We also analyzed CD206 levels that, while higher on chitosan-FPHS than on TCP, were not affected by Cp or DA variation (see **Fig. S2**, and **Table S1**).

The molecular mechanisms through which variations in Cp and DA of chitosan hydrogel may influence M $\Phi$  polarization remain to be elucidated. In our previous *in vivo* study<sup>10</sup> we had implanted chitosan-FPHS with low DA of 4%, which allowed for prolonged presence of M2 M $\Phi$  in and around the lesion site, beneficial for tissue regeneration, and compared it with another chitosan-FPHS with a very high DA of 38%. This latter formulation had elicited a very strong inflammatory reaction around the implant, and no regeneration was observed. A similar tendency for an attraction of anti-inflammatory M $\Phi$  towards a chitosan hydrogel implant with low DA (5%), but not higher DA (15%), had been described by others, albeit in a quite different experimental paradigm, a mouse subcutaneous air pouch model<sup>25</sup>.

On the one hand, it is well documented that the biomechanical properties of substrates, including hydrogels, will influence the physiology of adhering cells. In case of a chitosan hydrogel substrate, its stiffness/elasticity<sup>26,27</sup> is dependent on chitosan concentration (Cp), molar mass (i.e. chain length), and DA. Substrate stiffness, in turn, will impact adhesion, spreading, and motility of M $\Phi$ <sup>28,29,30</sup>. Together with particle size, these parameters will also influence phagocytic activity (stiffer particles being more readily engulfed<sup>31</sup>), which is particularly important in M2 M $\Phi$ <sup>32</sup>. Since the stiffness of a chitosan hydrogel is positively correlated with higher Cp<sup>16</sup> and/or lower DA<sup>33</sup> (for an estimation of corresponding Young modulus values, see<sup>34</sup>), results shown in Fig. 4 seem to suggest that stiffer chitosan hydrogel substrates eventually favor M2 over M1 polarization. However, if substrate stiffness plays a role, it should be kept in mind that the described tendency of chitosan-FPHS substrate to reduce M1 and/or enhance M2

M $\Phi$  marker expression (Fig. 4) may not be extrapolated to DA and Cp values beyond the range employed here. Indeed, the "neutral" tissue culture plastic or glass substrates obviously have much higher stiffness, yet induce higher M1 and lower M2 M $\Phi$  marker protein levels than chitosan-FPHS substrate. On the other hand, adhesion and spreading of M $\Phi$  on chitosan-FPHS will clearly be influenced by the chemical parameters of the latter (Cp, DA, chain length and entanglement), although the potentially involved cell surface receptors on M $\Phi$  have yet to be identified. The DA should be particularly important in this interaction since it influences the ionic charge/hydrophobicity of the biomaterial surface<sup>33,34</sup>.

### 3.4 M2 M $\Phi$ migrate preferentially onto low DA chitosan-FPHS

Intrigued by the high numbers of M2 M $\Phi$  colonizing chitosan-FPHS implants *in vivo* that contrasted with the quasi-absence of M1 M $\Phi$  within the implant (see our previous publication<sup>10</sup>, supplemental Fig. S3) we wanted to address the question whether chitosan-FPHS was a particularly well-suited substrate for M2 M $\Phi$ , and if so, whether this was dependent on the DA of chitosan (no M2 M $\Phi$  had been found in 38% DA implants). We used an insert culture system similar to the one depicted in Fig. 3b, but with greater pore diameter (8  $\mu$ m) allowing the cells seeded on the insert membrane to migrate through the pores onto glass coverslips treated either with PLL only, or covered with chitosan-FPHS with different DAs. Initial density of cells seeded on the insert membrane was equal for all cultures. While both M1 and M2 M $\Phi$  adhered and developed well on the PET (polyethylene terephthalate) insert membrane (see also Fig. 3), after 2 days of culture only M2 M $\Phi$  were found to have crossed the pores. The lack of amoeboid migration of M1 M $\Phi$  through the membrane pores (not shown) is likely due to their very strong substrate adhesion (here, to the membrane material), in accordance with their higher  $\beta$ 2-integrin expression compared to M2 M $\Phi$ <sup>35</sup>, and consistent also with their flat, "fried-egg" shape morphology in a 2-D environment *in vitro*. Since in our hands, LPS-induced M $\Phi$  could not be cultured for longer periods, transwell cultures were eventually performed with M2 polarized M $\Phi$  only. **Fig. 5** shows that after 4 days of culture, numerous M2 M $\Phi$  had migrated through the membrane and adhered both to PLL-coated (control), and chitosan-FPHS-coated glass coverslips. Cell numbers per area on PLL/glass and on 2% DA chitosan-FPHS were about equal, but M $\Phi$  morphology

differed between control and chitosan hydrogel substrates: while on PLL-treated glass, M2 M $\Phi$  exhibited an often multipolar shape with smooth borders, on 2% DA chitosan-FPHS cells had an overall more rounded morphology, with jaggy borders due to numerous F-actin positive protrusions (as seen in Fig. 1b). The higher the DA of the chitosan the less M2 M $\Phi$  were seen to invade the hydrogel: In comparison to 2% DA chitosan substrate, numbers of cells having migrated on 11%, and 15% DA chitosan were reduced by about 50%, and 85%, respectively. Their morphology with either filiform and jaggy, or very small round shape (almost lacking any cytosol) indicated an increasingly lower adhesiveness of the chitosan substrate. As outlined above, this effect may well be related to the chitosan-FPHS substrate becoming 'softer', i.e., less adhesive with increasing DA<sup>33,34</sup>. The reduced migration of M2 M $\Phi$  from the PET membrane onto higher DA chitosan-FPHS substrates may then be explained by a balance of substrate adhesiveness in favor of the PET membrane. Indeed, the effect is not observed in a simple adhesion assay (where cells are confronted to only one substrate), as M2 M $\Phi$  are capable of adhering to 15% DA as well as on low DA chitosan-FPHS or on PLL, as demonstrated in **Fig. S3**; however, on higher DA chitosan-FPHS the cells tend to aggregate, and spread less well than on low DA substrate.

The insert culture assay thus suggests that variations in the DA of chitosan-FPHS, while not significantly influencing M2 M $\Phi$  marker protein expression (in contrast to M1 M $\Phi$ , see Fig. 4), strongly affect substrate adhesion and morphology that are closely related to cell mobility, and may therefore have consequences for the invasion of anti-inflammatory M $\Phi$  into a chitosan-FPHS matrix implanted *in vivo*. It would be interesting in a future study to focus on the strength of macrophage adhesion in relation to chemical composition and stiffness of the chitosan biomaterial.

### 3.5 Implantation into rat SCI site of chitosan-FPHS with different DAs

Next, we investigated whether the results of the *in vitro* experiments described above could be translated to the situation *in vivo*, i.e. after implantation of chitosan-FPHS scaffolds with different parameters into a traumatic spinal cord lesion in adult rats. Thus, as illustrated in **Fig. 6**, 2 weeks post-lesion a chitosan-FPHS scaffold with a DA of 2% was massively invaded by CD206-positive M $\Phi$ , whereas only few inflammatory (CD86-positive) M $\Phi$  were found in the periphery of the not yet completely degraded

biomaterial implant. Inversely, a 15% DA chitosan-FPHS implant was colonized by only very few M2 M $\Phi$ , and a higher number of M1 M $\Phi$  were seen to closely surround the biomaterial. These results are in accordance with 2% DA chitosan hydrogel favoring M2 M $\Phi$  marker protein expression (Fig. 2), and allowing for efficient adhesion and spreading of M2 M $\Phi$  (Fig. 5), in contrast to chitosan with higher DA that in addition, rather stimulates polarization towards the M1 phenotype. We may add that inflammatory M1 M $\Phi$  are rarely observed within a chitosan-FPHS implant, be it 2% or 15% DA (Fig. 6), or even 38% DA chitosan, as we previously demonstrated<sup>10</sup>. In the light of our *in vitro* assays described above, the results shown in Fig. 6 suggest that circulating "naïve" monocytes that invade a low DA chitosan-FPHS implant may be preferentially polarized to become anti-inflammatory M $\Phi$ , while at the same time the polarization state of M1 pre-polarized M $\Phi$  coming into contact with the implant would be reduced, weakening the feedback loop of inflammatory cytokine secretion that otherwise would attract even more M1 M $\Phi$  to the lesion site. Nevertheless, the reason for the non-colonization of chitosan-FPHS implants by M1 M $\Phi$  remains to be elucidated, given that *in vitro* these cells are perfectly capable of adhering and proliferating on chitosan-FPHS (Fig. 1).

### 3.6 Use of the *in vitro* assay system for other biomaterials

Finally, we used the same experimental setup to investigate the impact on inflammation of two other compounds having shown an effect on nervous tissue regeneration in various *in vitro* and *in vivo* conditions: (i) Chitosan-derived oligosaccharides (COS), and (ii) polyethylene glycol (PEG). Thus, an important parameter of chitosan hydrogel to be implanted *in vivo* is its dispersion/degradation with time, not least to make place for the reconstruction of a functional tissue (neural or other). In addition to its breakdown by phagocytic activity of M $\Phi$  and other inflammatory cells, chitosan may be degraded by certain enzymes, notably lysozyme present in human blood, and diverse lipases<sup>36</sup>. Degradation velocity is mainly dependent on the DA of chitosan, increasing with increasing DA<sup>37</sup>, except for very high DA values (approaching that of chitin, >90 % DA); the most rapid degradation is observed for DA values between 30-70%<sup>38</sup>. Thus, it has been suggested that part of the chitosan hydrogel effects seen *in vivo* are likely due to its oligomeric degradation products (for review<sup>39</sup>).

Chito-OligoSaccharides (COS), chemically or enzymatically prepared from chitosan, have been reported to exhibit a number of properties that may well be interesting for nervous tissue regeneration, although shown so far only for peripheral nervous system: they are capable of attenuating oxidative stress<sup>40</sup>, promoting Schwann cell proliferation<sup>41,42</sup>, and enhancing neurite outgrowth from dorsal root ganglion neurons *in vitro*<sup>43</sup>. Taken together, these properties appear to favor peripheral nerve regeneration<sup>44</sup>. In addition, the presence of COS at a peripheral nerve lesion site may also influence M $\Phi$ -related microenvironments, triggering inflammatory M $\Phi$  invasion by transiently enhancing pro-inflammatory cytokine expression in Schwann cells<sup>45</sup>.

We show here that supplementing the culture medium with 1 mg/mL of a specific formulation of commercially available COS ( $M_w \leq 1500$  g/mol, DA  $\sim 8,5\%$ ) shifted M $\Phi$  marker protein expression towards a more inflammatory phenotype, both on tissue culture plastic, and on chitosan substrate (**Fig. 7**). Moreover, immunocytochemical staining of M $\Phi$  cultures with the proliferation marker Ki67 shows that COS-treated M2 M $\Phi$  were mitotically less active, and exhibited a more rounded morphology, closer to that of typical M1 M $\Phi$  (**Fig. 8**). At first sight, these results seemed contradictory to other studies reporting a generally rather anti-inflammatory activity of both chitosan (in agreement with our own findings), and its low molecular weight derivatives. In particular, COS with a molecular weight of  $\sim 5000$ - $10,000$  g/mol and a DA of the source chitosan of 10% were shown to reduce inflammatory cytokine production in LPS-induced RAW264.7 (M $\Phi$ -like) cells, and in a LPS/ $\beta$ -amyloid-stressed astrocytoma cell line, as well as *in vivo* in a mouse paw edema model<sup>46-48</sup>. In fact, Lee *et al.*<sup>47</sup> had determined how COS activity depended on DA, molecular weight, and concentration; thus, increased iNOS levels were found with COS of higher DA and/or lower molecular weight (between 1000 and 5000 g/mol). While the particular COS used here did raise iNOS levels when combined with chitosan substrate, they also enhanced arginase-1 expression by M2 M $\Phi$  (albeit to a lesser extent than chitosan-FPHS; Fig. 7). While our data illustrate that COS indeed exert a strong impact on M $\Phi$  polarization, different types of COS with regard to their DA and molecular weight should thus be tested to obtain a specific pro- or anti-inflammatory effect.

In view of the rather strong effects on M $\Phi$  polarization of chitosan-FPHS (**Fig. 2**), and COS (**Fig. 7**), we wanted to know whether chitosan-FPHS substrate, COS, or a combination of both, would suffice to drive *in vitro* polarization of "naïve" monocytes

towards an inflammatory or anti-inflammatory M $\Phi$  phenotype. To this end, we cultured monocytes without addition of polarizing factors on a substrate of chitosan hydrogel particles with two different DAs, 2% and 15%. As illustrated in **Fig. 9**, neither 2%, nor 15% DA chitosan hydrogel particles induced any measurable M1 marker protein (iNOS) expression. However, upon addition of the above formulation of COS to the medium, alone or in combination with chitosan (15% DA), some faint iNOS expression was observed (note that iNOS levels in non-LPS induced, only COS-treated monocytes are in fact orders of magnitude lower than those in M1-polarized M $\Phi$  and cannot be directly compared; see Fig. 9 middle panel, and Fig. 2). Culturing monocytes on chitosan substrate (in particular 2% DA chitosan) elicited faint arginase-1 expression that was reduced in the presence of 8.5% DA/Mw 1500 COS. M2 marker protein CD206 was undetectable under all conditions. We conclude from these experiments that low DA chitosan substrate has a small but measurable effect driving monocytes towards an M2a phenotype, whereas addition of the specific COS used here (MW  $\leq$ 1500, DA  $\sim$ 8,5%) rather favored M1 polarization.

We also compared the M $\Phi$ -polarizing effect of chitosan hydrogel particles to another polymer having shown very promising results in a similar SCI paradigm, i.e. Poly-Ethylene Glycol (PEG; for rodent SCI<sup>49,50</sup>; for dog SCI<sup>51</sup>). Among other features, PEG has a membrane-resealing (fusogenic) capacity that may obviously be beneficial after a traumatic lesion to nervous system<sup>52</sup>, has long been known to boost mammalian cell proliferation, and can be used as serum replacement for cell culture<sup>53</sup>. In a therapeutic approach to SCI, PEG can be employed either non-modified, or cross-linked to yield hydrogels with tunable properties (for review<sup>54</sup>). The non-crosslinked PEG-600 used for example by Estrada and coworkers<sup>49</sup> being liquid at 37°C, it cannot be used as culture substrate, but was diluted in the culture medium at different concentrations. As seen in **Fig. 10**, supplementation of the culture medium with increasing amounts of PEG-600 (from 1% onwards) resulted in a drastic reduction of specific marker protein expression for both M1 and M2 M $\Phi$ , becoming non detectable at a concentration of 5%, whereas low PEG-600 concentrations (<0.2%) increased both iNOS, and Arg-1 expression in M1, and M2 polarized M $\Phi$ , respectively. At concentrations of 20% and higher M $\Phi$  detached from the substrate and died, most likely due to osmotic shock (not shown). Thus, in contrast to chitosan hydrogel particles as used in<sup>10</sup>, non-crosslinked PEG-600 does not

appear to specifically drive M $\Phi$  polarization towards a more anti-inflammatory type *in vitro*.

## 4. DISCUSSION

Today, it is more or less consensus among researchers and clinicians that novel therapeutic approaches to traumatic SCI should be designed around a biomaterial scaffold replacing damaged or lost extracellular matrix. The scaffold material should, ideally, be bio-compatible (non-toxic), allow for deposition of new matrix material, favor cell attachment, proliferation and maturation (notably of endothelial cells ensuring revascularization), as well as growth of axons or axon collaterals, while at the same time being gradually degraded, making place for newly forming spinal tissue<sup>10;54-60</sup>.

As mentioned above, one of the major problems of SCI is the associated uncontrolled inflammation that spreads into neighboring segments creating further damage, and may persist almost indefinitely<sup>2,6,7,56,61-63</sup>. As we have shown<sup>10</sup>, implantation into the lesion site of a defined formulation of chitosan-FPHS exhibited a clear anti-inflammatory effect, as M1 M $\Phi$  density was reduced, whereas numerous M2 M $\Phi$  persisted within and around the primary lesion for several weeks, instead of disappearing after about one week post-lesion.

In the light of the above considerations, chitosan-FPHS appears an ideal starting material for creating a bio-scaffold to be implanted into a spinal cord lesion. Moreover, chitosan hydrogel can also be formed to tubes, sponges or other, quite sophisticated structures, as well as be used for co-implantation of stem cells, or controlled release of trophic factors or neuroprotective agents<sup>14,17,20,64,65</sup>. Since it is not possible, both from ethical, as well as experimental points of view, to test many different modifications of a biomaterial by implanting each of them *in vivo*, pertinent *in vitro* assays are needed to help narrowing down the choice to a few, promising formulations. Thus, in addition to being a bio-compatible and bio-degradable extracellular matrix replacement allowing for cell attachment and axon regrowth (such as chitosan-FPHS), the "ideal" biomaterial would contribute to regulate the balance between inflammatory events indispensable

shortly after SCI, and the activity of diverse subtypes of anti-inflammatory M $\Phi$  that play a major role in tissue reconstruction.

The work presented here should help assess and fine-tune the inflammatory properties of an implantable bioscaffold *via* relatively rapid and straightforward *in vitro* assays: *i)* Analyzing the expression levels of typical M1 or M2 marker proteins extracted from cultures of M $\Phi$  (or unpolarized monocytes) grown on chitosan-FPHS or other scaffold materials shows whether the material itself influences M $\Phi$  polarization towards a more inflammatory, or anti-inflammatory subtype, and how this effect may be modulated by variations in the specific formulation of the biomaterial. Our approach based on SDS-electrophoresis and Western blotting could principally be replaced by other detection methods (such as ELISA), but it may be difficult to retrieve high enough protein concentrations from cells growing on and within a 3-dimensional, porous substrate (like chitosan-FPHS) using a "soft" extraction method. *ii)* The insert culture system indicates whether the polarizing effect is contact-dependent, since changes in M $\Phi$  polarization could also be due to e.g., absorption by a hydrogel of polarizing factors from the culture medium, or liberation of soluble degradation products exhibiting a polarizing activity. *iii)* The migration assay giving M $\Phi$  the choice between two different substrates, the semi-permeable membrane and the biomaterial underneath, shows whether the substrate properties of the particular biomaterial, namely cell adherence, are appropriate for invasion by M $\Phi$ .

## 5. CONCLUSION

We show here by different *in vitro* assays that chitosan-FPHS with appropriate physico-chemical characteristics exerts a strong anti-inflammatory effect that is dependent on direct contact between biomaterial and macrophages. Thus, in comparison to a control culture (on a glass or plastic substrate) the expression level of M1 M $\Phi$  marker protein iNOS is strongly decreased on chitosan-FPHS with low DA and/or higher concentration (Cp), which may be partly correlated with relative stiffness values of the hydrogel; another part should be attributed to the chemical characteristics of chitosan, since also most soluble low molecular weight isoforms (COS) display an anti-inflammatory

activity<sup>45-47</sup>. Inversely, expression levels of specific M2 marker proteins are increased on chitosan-FPHS, but are less affected by changes in DA or Cp. Moreover, M2 MΦ adhere, spread, and proliferate well on a low DA (below 6%) chitosan-FPHS, both *in vitro* and *in vivo*, whereas inflammatory M1 MΦ rarely invade chitosan-FPHS implants *in vivo*. M1 MΦ, while capable of adhering to chitosan-FPHS *in vitro*, exhibit a lower migration capacity than M2 MΦ<sup>35</sup> and avoid migrating on chitosan-FPHS substrate if given the choice. Thus, the *in vitro* data presented here can be correlated to the *in vivo* situation of chitosan-FPHS implantation into a spinal cord lesion, where the biomaterial is massively invaded by M2 MΦ, provided a low DA chitosan is used (in agreement with our previously published data<sup>10</sup>). Finally, as shown here for low molecular weight breakdown products of chitosan (COS) and for PEG, our *in vitro* experimental setup is also well suited to study the impact on inflammation of other biomaterial formulations, or combinations of such biomaterials.

### **Declaration of conflicting interests**

The authors declared no potential conflicts of interest with respect to the research, authorship, and/or publication of this article.

### **Funding**

The present work was supported by SATT-Lutech (Société d'Accélération du Transfert de Technologies - Lutech), Paris.

## References

1. Koh TJ, DiPietro LA. Inflammation and wound healing: the role of the macrophage. *Expert Rev Mol Med*. 2011;13:e23.
2. Gensel JC, Zhang B. Macrophage activation and its role in repair and pathology after spinal cord injury. *Brain Res*. 2015;1619:1-11.
3. David S, Greenhalgh AD, Kroner A. Macrophage and microglial plasticity in the injured spinal cord. *Neuroscience*. 2015;307:311-318.
4. Kigerl KA, Gensel JC, Ankeny DP, et al. Identification of two distinct macrophage subsets with divergent effects causing either neurotoxicity or regeneration in the injured mouse spinal cord. *J Neurosci*. 2009;29(43):13435-13444.
5. Hawthorne AL, Popovich PG. Emerging concepts in myeloid cell biology after spinal cord injury. *Neurotherapeutics*. 2011;8(2):252-261.
6. Ren Y, Young W. Managing inflammation after spinal cord injury through manipulation of macrophage function. *Neural Plast*. 2013;945034.
7. Zhou X, He X, Ren Y. Function of microglia and macrophages in secondary damage after spinal cord injury. *Neural Regen Res*. 2014 9(20):1787-1795.
8. Brennan FH, Popovich PG. Emerging targets for reprogramming the immune response to promote repair and recovery of function after spinal cord injury. *Curr Opin Neurol*. 2018; 31(3):334-344.
9. Orr MB, Gensel JC. Spinal Cord Injury Scarring and Inflammation: Therapies Targeting Glial and Inflammatory Responses. *Neurotherapeutics*. 2018;15(3):541-553.
10. Chedly J, Soares S, Montembault A, et al. Physical chitosan microhydrogels as scaffolds for spinal cord injury restoration and axon regeneration. *Biomaterials*. 2017; 138:91-107.
11. Chen B, Bohnert D, Borgens RB, Cho Y. Pushing the science forward: chitosan nanoparticles and functional repair of CNS tissue after spinal cord injury. *J Biol Eng*. 2013;7:15.
12. Huang C, Chen R, Ke Q, et al. Electrospun collagen-chitosan-TPU nanofibrous scaffolds for tissue engineered tubular grafts. *Colloids Surf B Biointerfaces* 2011;82: 307-315.
13. Aduba DC, Yang H. Polysaccharide Fabrication Platforms and Biocompatibility Assessment as Candidate Wound Dressing Materials. *Bioengineering (Basel)*. 2017;4: 1.
14. Rao JS, Zhao C, Zhang A, et al. NT3-chitosan enables de novo regeneration and functional recovery in monkeys after spinal cord injury. *Proc Natl Acad Sci U S A*. 2018; 115(24):E5595-E5604.

15. Freier T, Montenegro R, Shan Koh H, Shoichet MS. Chitin-based tubes for tissue engineering in the nervous system. *Biomaterials*. 2005;26(22):4624-4632.
16. Fiamingo A, Montembault A, Boitard SE, et al. Chitosan Hydrogels for the Regeneration of Infarcted Myocardium: Preparation, Physicochemical Characterization, and Biological Evaluation. *Biomacromolecules*. 2018;17(5):1662-1672.
17. Ladet SG, Tahiri K, Montembault AS, Domard AJ, Corvol MT. Multi-membrane chitosan hydrogels as chondrocytic cell bioreactors. *Biomaterials*. 2011;32(23):5354-5364.
18. Yang Z, Zhang A, Duan H, et al. NT3-chitosan elicits robust endogenous neurogenesis to enable functional recovery after spinal cord injury. *Proc Natl Acad Sci U S A*. 2015; 112(43):13354-13359.
19. Bozkurt G, Mothe AJ, Zahir T, et al. Chitosan channels containing spinal cord-derived stem/progenitor cells for repair of subacute spinal cord injury in the rat. *Neurosurgery*. 2010;67(6):1733-1744.
20. Hu X, Zhou X, Li Y, et al. Application of stem cells and chitosan in the repair of spinal cord injury. *Int J Dev Neurosci*. 2019;76:80-85.
21. Vachoud L, Zydowicz N, Domard A. Physicochemical behaviour of chitin gels. *Carbohydr Res*. 2000;326:295-304.
22. Zhang X, Goncalves R, Mosser DM. The isolation and characterization of murine macrophages. *Curr Protoc Immunol*. 2008; Chapter 13:Unit 14.1.
23. von Boxberg Y. Protein analysis on two-dimensional polyacrylamide gels in the femtogram range: use of a new sulfur-labeling reagent. *Anal Biochem*. 1988;169(2): 372-375.
24. Roszer T. Understanding the Mysterious M2 Macrophage through Activation Markers and Effector Mechanisms. *Mediators Inflamm*. 2015;2015:816460.
25. Vasconcelos DP, Fonseca AC, Costa M, et al. Macrophage polarization following chitosan implantation. *Biomaterials*. 2013;34(38):9952-9959.
26. Blakney AK, Swartzlander MD, Bryant SJ. The effects of substrate stiffness on the in vitro activation of macrophages and in vivo host response to poly(ethylene glycol)-based hydrogels. *J Biomed Mater Res A*. 2012;100(6):1375-1386.
27. Sacco P, Cok M, Asaro F, Paoletti S, Donati I. The role played by the molecular weight and acetylation degree in modulating the stiffness and elasticity of chitosan gels. *Carbohydr Polym*. 2018;196:405-413.
28. McWhorter FY, Wang T, Nguyen P, Chung T, Liu WF. Modulation of macrophage phenotype by cell shape. *Proc Natl Acad Sci U S A*. 2013;110(43):17253-17258.
29. McWhorter FY, Davis CT, Liu WF. Physical and mechanical regulation of macrophage phenotype and function. *Cell Mol Life Sci*. 2015;72(7):1303-1316.

30. Fereol S, Fodil R, Laurent VM, et al. Prestress and adhesion site dynamics control cell sensitivity to extracellular stiffness. *Biophys J*. 2009;96(5):2009-2022.
31. Bueter CL, Lee CK, Rathinam VA, et al. Chitosan but not chitin activates the inflammasome by a mechanism dependent upon phagocytosis. *J Biol Chem*. 2011; 286(41):35447-35455.
32. Schulz D, Severin Y, Zanotelli VRT, Bodenmiller B. In-depth characterization of monocyte-derived macrophages using a mass cytometry-based phagocytosis assay. *Sci Rep*. 2019;9(1):1925.
33. Rami L, Malaise S, Delmond S, et al. Physicochemical modulation of chitosan-based hydrogels induces different biological responses: interest for tissue engineering. *J Biomed Mater Res A*. 2014;102(10):3666-3676.
34. Benbouali A, Montembault A, David L, et al. Nanoscale mechanical properties of chitosan hydrogels as revealed by AFM. *Progr in Biomat*. 2020;9:187-201.
35. Cui K, Ardell CL, Podolnikova NP, Yakubenko VP. Distinct migratory properties of M1, M2, and resident macrophages are regulated by  $\alpha_D\beta_2$  and  $\alpha_M\beta_2$  integrin-mediated adhesion. *Front Immunol*. 2018;9:2650.
36. Martins AM, Santos MI, Azevedo HS, Malafaya PB, Reis RL. Natural origin scaffolds with in situ pore forming capability for bone tissue engineering applications. *Acta Biomater*. 2008;4(6):1637-1645.
37. Ren D, Yi H, Wang W, Ma X. The enzymatic degradation and swelling properties of chitosan matrices with different degrees of N-acetylation. *Carbohydr Res*. 2005;340(15):2403-2410.
38. Freier T, Koh HS, Kazazian K, Shoichet MS. Controlling cell adhesion and degradation of chitosan films by N-acetylation. *Biomaterials*. 2005;26(29):5872-5878.
39. Muanprasat C, Chatsudthipong V. Chitosan oligosaccharide: Biological activities and potential therapeutic applications. *Pharmacol Ther*. 2017;170:80-97.
40. Liu HT, Li WM, Xu G, et al. Chitosan oligosaccharides attenuate hydrogen peroxide-induced stress injury in human umbilical vein endothelial cells. *Pharmacol Res*. 2009; 59(3):167-175.
41. Jiang M, Cheng Q, Su W, et al. The beneficial effect of chitooligosaccharides on cell behavior and function of primary Schwann cells is accompanied by up-regulation of adhesion proteins and neurotrophins. *Neurochem Res*. 2014;39(11):2047-2057.
42. Wang Y, Zhao Y, Sun C, et al. Chitosan Degradation Products Promote Nerve Regeneration by Stimulating Schwann Cell Proliferation via miR-27a/FOXO1 Axis. *Mol Neurobiol*. 2016;53(1): 28-39.

43. Jiang M, Guo Z, Wang C, et al. Neural activity analysis of pure chito-oligomer components separated from a mixture of chitooligosaccharides. *Neurosci Lett.* 2014; 581:32-36.
44. Jiang M, Zhuge X, Yang Y, Gu X, Ding F. The promotion of peripheral nerve regeneration by chitooligosaccharides in the rat nerve crush injury model. *Neurosci Lett.* 2009;454(3):239-243.
45. Zhao Y, Wang Y, Gong J, et al. Chitosan degradation products facilitate peripheral nerve regeneration by improving macrophage-constructed microenvironments. *Biomaterials.* 2017;134:64-77.
46. Kim MS, Sung MJ, Seo SB, et al. Water-soluble chitosan inhibits the production of pro-inflammatory cytokine in human astrocytoma cells activated by amyloid beta peptide and interleukin-1beta. *Neurosci Lett.* 2002;321(1-2):105-109.
47. Lee SH, Senevirathne M, Ahn CB, Kim SK, Je JY. Factors affecting anti-inflammatory effect of chitooligosaccharides in lipopolysaccharides-induced RAW264.7 macrophage cells. *Bioorg Med Chem Lett.* 2009;19(23):6655-6658.
48. Fernandes JC, Spindola H, de Sousa V, et al. Anti-inflammatory activity of chitooligosaccharides in vivo. *Mar Drugs.* 2010;8(6):1763-1768.
49. Estrada V, Brazda N, Schmitz C, et al. Long-lasting significant functional improvement in chronic severe spinal cord injury following scar resection and polyethylene glycol implantation. *Neurobiol Dis.* 2014;67:165-179.
50. Brazda N, Estrada V, Voss C, et al. Experimental strategies to bridge large tissue gaps in the Injured spinal cord after acute and chronic lesion. *J Vis Exp.* 2016;(110):e53331.
51. Kim CY, Hwang IK, Kim H, et al. Accelerated recovery of sensorimotor function in a dog submitted to quasi-total transection of the cervical spinal cord and treated with PEG. *Surg Neurol Int.* 2016;7(Suppl 24):S637-40.
52. Borgens RB, Shi R. Immediate recovery from spinal cord injury through molecular repair of nerve membranes with polyethylene glycol. *FASEB J.* 2000;14(1):27-35.
53. Kitano K, Ichimori Y, Sawada H, et al. Effective production of anti-tetanus toxoid and anti-HBsAg human monoclonal antibodies by serum-free culture of hybridomas. *Cytotechnology.* 1991;5(Suppl 2):S53-74.
54. Lu X, Perera TH, Aria AB, Callahan LAS. Polyethylene glycol in spinal cord injury repair: a critical review. *J Exp Pharmacol.* 2018;10:37-49.
55. Assunção-Silva RC, Gomes ED, Sousa N, Silva NA, Salgado AJ. Hydrogels and cell based therapies in spinal cord injury regeneration. *Stem Cells Int.* 2015; 2015:948040.
56. Haggerty AE, Oudega M. Biomaterials for spinal cord repair. *Neurosci Bull* 2013;29(4): 445-459.

57. Ham TR, Leipzig ND. Biomaterial strategies for limiting the impact of secondary events following spinal cord injury [editorial]. *Biomed Mater*. 2018;13(2):024105.
58. Kim M, Park SR, Choi BH. Biomaterial scaffolds used for the regeneration of spinal cord injury (SCI). *Histol Histopathol*. 2014;29(11):1395-1408.
59. Krishna V, Konakondla S, Nicholas J, et al. Biomaterial-based interventions for neuronal regeneration and functional recovery in rodent model of spinal cord injury: a systematic review. *J Spinal Cord Med*. 2013;36(3):174-190.
60. Madigan NN, McMahon S, O'Brien T, Yaszemski MJ, Windebank AJ. Current tissue engineering and novel therapeutic approaches to axonal regeneration following spinal cord injury using polymer scaffolds. *Respir Physiol Neurobiol*. 2009;169(2):183-199.
61. Sakiyama-Elbert S, Johnson PJ, Hodgetts SI, Plant GW, Harvey AR. Scaffolds to promote spinal cord regeneration. *Handb Clin Neurol*. 2012;109:575-594.
62. Donnelly DJ, Popovich PG. Inflammation and its role in neuroprotection, axonal regeneration and functional recovery after spinal cord injury. *Exp Neurol*. 2008;209(2):378-388.
63. Schwab JM, Zhang Y, Kopp MA, Brommer B, Popovich PG. The paradox of chronic neuroinflammation, systemic immune suppression, autoimmunity after traumatic chronic spinal cord injury. *Exp Neurol*. 2014;258:121-129.
64. Shechter R, Schwartz M. Harnessing monocyte-derived macrophages to control central nervous system pathologies: no longer 'if' but 'how'. *J Pathol*. 2013;229(2):332-346.
65. Li X, Yang Z, Zhang A, Wang T, Chen W. Repair of thoracic spinal cord injury by chitosan tube implantation in adult rats. *Biomaterials*. 2009;30(6):1121-1132.
66. Sun Y, Yang C, Zhu X, et al. 3D printing collagen/chitosan scaffold ameliorated axon regeneration and neurological recovery after spinal cord injury. *J Biomed Mater Res A*. 2019;107(9):1898-1908.

## Figure legends

**Fig 1: Macrophage culture on chitosan-FPHS substrate.** **a:** Chitosan-FPHS particles (2% DA, 2.5% Cp) in suspension (left, dark-field image), and as substrate layer with rough surface on tissue culture plastic, made of densely packed particles after evaporation of excess water from the suspension (right, phase contrast image). **b:** Mouse monocyte-derived M1 (top row) and M2 (bottom row) M $\Phi$  cultured on different substrates. Left: phase contrast images of M $\Phi$  on tissue culture plastic (can serve as morphological control for M1/M2 polarization); middle and right: fluorescence-labeled M $\Phi$  on PLL-coated (middle), and on chitosan-FPHS-coated glass coverslips (right); phalloidin/DAPI staining. Note the change in morphology of M $\Phi$  between a "neutral" substrate, and chitosan-FPHS. Scale bars: 100 $\mu$ m for all images in a, and b, respectively.

**Fig 2: Impact of chitosan-FPHS substrate (2% DA, 2.5% Cp) on M $\Phi$  polarization *in vitro*.** Compared to M $\Phi$  growing on tissue culture plastic (TCP), on chitosan-FPHS substrate inflammatory M1 marker protein expression (iNOS) is reduced, whereas that of anti-inflammatory M2 marker proteins (Arginase-1, CD206) is enhanced (expression on TCP is set arbitrarily to "1"). M $\Phi$  had been pre-polarized by IFN-gamma/LPS, or IL-4, respectively.  $\beta$ -actin expression is used for reference. Marker protein antibodies are specific, since they do not react with protein extracts from non-polarized (n.p.), "naive" monocytes ("M0"). Note that Arg-1 and actin bands were always revealed simultaneously on the same membrane, the actin band (43 kDa) being situated above that of Arg-1 (35 kDa); the apparent molecular weight of iNOS is ~130 kDa, that of CD206 ~175 kDa. n=4, \*\*\* p=0,0001, \*\*\*\*p<0,0001 (Student's t-test).

**Fig 3: Polarizing effect of chitosan-FPHS depends on direct contact with M $\Phi$ .** In insert cultures (3.0  $\mu$ m pores), in which M $\Phi$  are not in direct contact with chitosan-FPHS substrate, the latter has no influence on M1 or M2 M $\Phi$  marker protein expression. The sketch shows the different culture types in cross-section: (a) M $\Phi$  (orange) grow on the insert membrane (red: culture medium), no chitosan present; (b) a chitosan particle film (green) is generated on the bottom of the well, and M $\Phi$  seeded within the insert are separated from the chitosan layer by the porous membrane; (c) M $\Phi$  are seeded on the bottom of the well and a dense chitosan-FPHS slurry is added into the insert.

**Fig 4: Influence of chitosan concentration (Cp) and DA of the hydrogel particle substrate on MΦ polarization.** For statistical evaluation the values obtained for one specific condition were arbitrarily set to 1. **M1 MΦ (top):** There is a tendency of decreasing iNOS levels with increasing Cp (n=4), while in contrast, increasing the DA leads to significantly increasing iNOS expression that almost reaches control (TCP) values for 11% and 15% DA (n=5). **M2 MΦ (bottom):** M2 marker protein expression exhibits a tendency to increase with increasing Cp (n=4), while being very little, if at all affected by changes in DA (n=3). Higher DA chitosans (6%, 11%, 15%) were prepared by reacylation of 2% DA chitosan. Note that the observed impact of chitosan-FPHS on MΦ polarization may not be extrapolated to much higher Cp or DA values. One-way ANOVA with Tukey's post-hoc test, \* p<0.05, \*\* p<0.01, \*\*\* p<0.001, \*\*\*\* p<0.0001 (see also Figs. S1, S2, and Table S1).

**Fig 5: Transwell cultures of M2 MΦ.** Migration of M2 MΦ through ThinCert membranes (8.0 μm pores) after 4 days of culture, onto control coverslips (PLL/glass), or on chitosan-FPHS layers made of 2%, 11% or 15% DA chitosan (M1 MΦ did not migrate through the membrane). Note the differences in cell shape between MΦ having migrated onto PLL/glass vs. a substrate made of 2% DA chitosan-FPHS, and the decreasing numbers and changing morphologies of M2 MΦ migrating on chitosan-FPHS with higher DA values (see also Fig. S3). Scale bar: 100μm.

**Fig.6: MΦ phenotype invading chitosan-FPHS *in vivo* depends on its DA.** A dorsal bilateral hemisection of adult rat spinal cord (thoracic level T8-T9) was performed, and the lesion site was either filled with a dense slurry of 2% DA, or 15% DA chitosan-FPHS, or left untreated (lesion only). All animals had a locomotor score of "0" on the BBB scale the day following the lesion. Immunohistochemical staining of horizontal sections of the injured region 2 weeks after the lesion shows that 2% DA chitosan-FPHS is exclusively invaded by M2 MΦ (CD206 labeling, green), a few M1 MΦ (CD86 labeling, red) are seen surrounding the lesion site in some distance. Inversely, only few M2 MΦ are present in a 15% DA chitosan-FPHS implant, and higher numbers of M1 MΦ found close to the lesion border, without entering the implant. Note that the biomaterial-implanted lesion site is colonized by a high number of cells that will ultimately restore a neural tissue (DAPI

nuclear staining, particularly dense at the lesion border). Without chitosan-FPHS implantation, a lesion cavity forms due to tissue necrosis (here at 3 weeks post-injury) surrounded by numerous M1, and some M2 M $\Phi$ . Scale bar: 300 $\mu$ m.

**Fig 7: Polarizing effect of chito-oligosaccharides (COS).** Addition of a particular type of COS (MW  $\leq$ 1500, DA  $\sim$ 8,5%; 1 mg/mL) to the medium slightly enhances iNOS expression of M1 M $\Phi$  grown on chitosan-FPHS (not significant; n=4). In contrast, in cultures of M2 M $\Phi$  CD206 expression is significantly reduced by the addition of COS on both TCP (Ctrl), and on chitosan substrate (n=4). Presence of COS significantly enhances arginase-1 expression on TCP, but clearly reduces arginase-1 levels on chitosan substrate. TCP (Ctrl): tissue culture plastic; COS: COS addition to culture on TCP; Chito: culture on chitosan-FPHS; Chito/COS (C+C): COS addition to culture on chitosan-FPHS. ANOVA with Tukey's post-hoc test; \* p<0.05, \*\* p<0.01, \*\*\* p<0.001, \*\*\*\* p<0.0001; see also Table S2.

**Fig 8: COS treatment alters M $\Phi$  morphology and proliferation rate.** M $\Phi$  cultures grown on PLL-treated glass coverslips, stained with proliferation marker Ki67 antibody (red), phalloidin (F-actin, green), and DAPI (nuclei, blue). M1 M $\Phi$  show a rounded morphology, and weak proliferation. In comparison, M2 M $\Phi$  exhibit a much stronger mitotic activity, which is greatly reduced upon addition of COS. Also note the change in morphology between COS-treated and -untreated M2 M $\Phi$ . Scale bar: 100 $\mu$ m.

**Fig 9: Impact of chitosan-FPHS substrate and COS on non-polarized monocytes.** Neither 2% nor 15% DA chitosan-FPHS substrate induce expression of M1 marker protein iNOS by naïve monocytes, but a faint iNOS expression is observed after addition of COS to the culture medium (1mg/mL), even slightly enhanced in the presence of 15% DA chitosan-FPHS. However, the absolute levels of iNOS expression by naïve monocytes induced by COS addition are in fact very low, and cannot be directly compared with those observed in LPS-induced M1 M $\Phi$  (middle panel: the revelation reaction was allowed to continue until appearance of a faint iNOS band from the COS-only polarized sample). In contrast, chitosan-FPHS (both 2% and 15% DA) culture substrates are seen to elicit some low level arginase-1 (but not CD206) expression from naïve monocytes

that is slightly diminished by addition of COS. TCP: tissue culture plastic; Chito+COS: 15% DA chitosan plus COS addition.

**Fig 10: PEG-600 has no specific impact on M $\Phi$  polarization in culture.** While low concentrations of PEG (0.2%) in the medium appear to enhance marker protein expression at least for M2, and probably also M1 M $\Phi$  (iNOS levels being comparable to those obtained on TCP, Arg-1 levels to those on chitosan-FPHS substrate), higher concentrations then gradually provoke a reduction in both M1, and M2 marker protein expression.

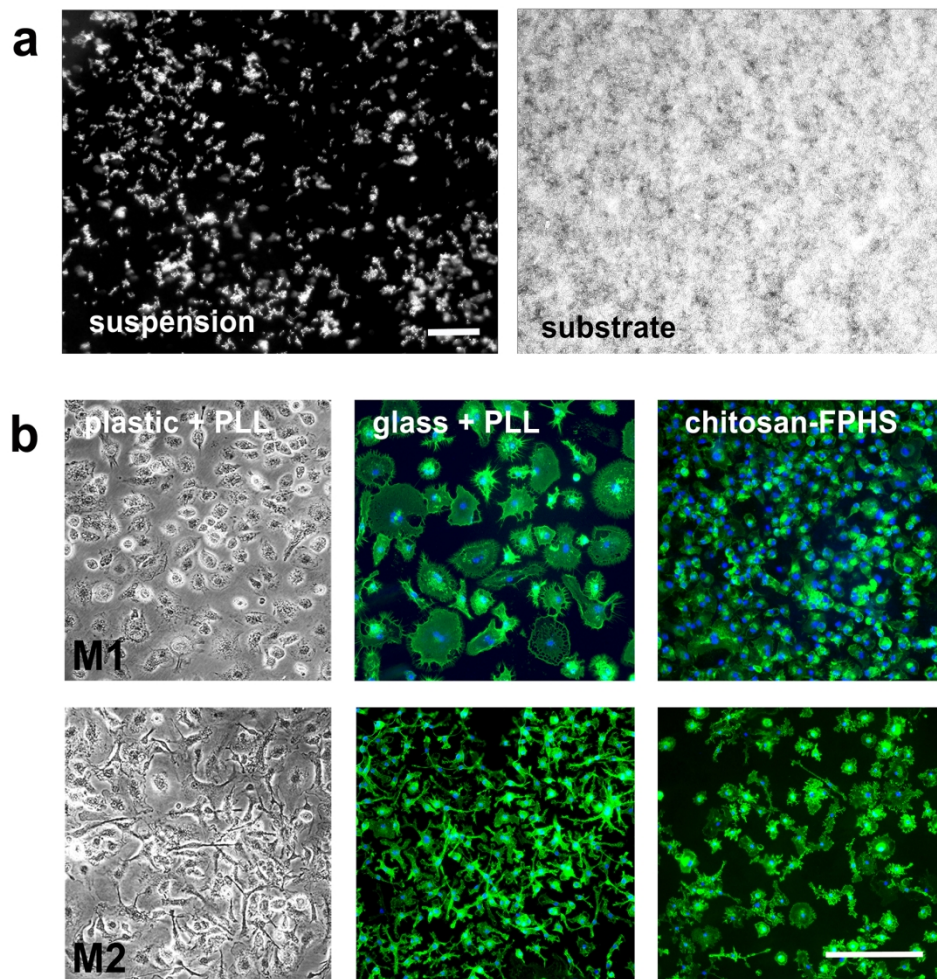


Fig 1: Macrophage culture on chitosan-FPHS substrate. a: Chitosan-FPHS particles (2% DA, 2.5% Cp) in suspension (left, dark-field image), and as substrate layer with rough surface on tissue culture plastic, made of densely packed particles after evaporation of excess water from the suspension (right, phase contrast image). b: Mouse monocyte-derived M1 (top row) and M2 (bottom row) M $\Phi$  cultured on different substrates. Left: phase contrast images of M $\Phi$  on tissue culture plastic (can serve as morphological control for M1/M2 polarization); middle and right: fluorescence-labeled M $\Phi$  on PLL-coated (middle), and on chitosan-FPHS-coated glass coverslips (right); phalloidin/DAPI staining. Note the change in morphology of M $\Phi$  between a "neutral" substrate, and chitosan-FPHS. Scale bars: 100 $\mu$ m for all images in a, and b, respectively.

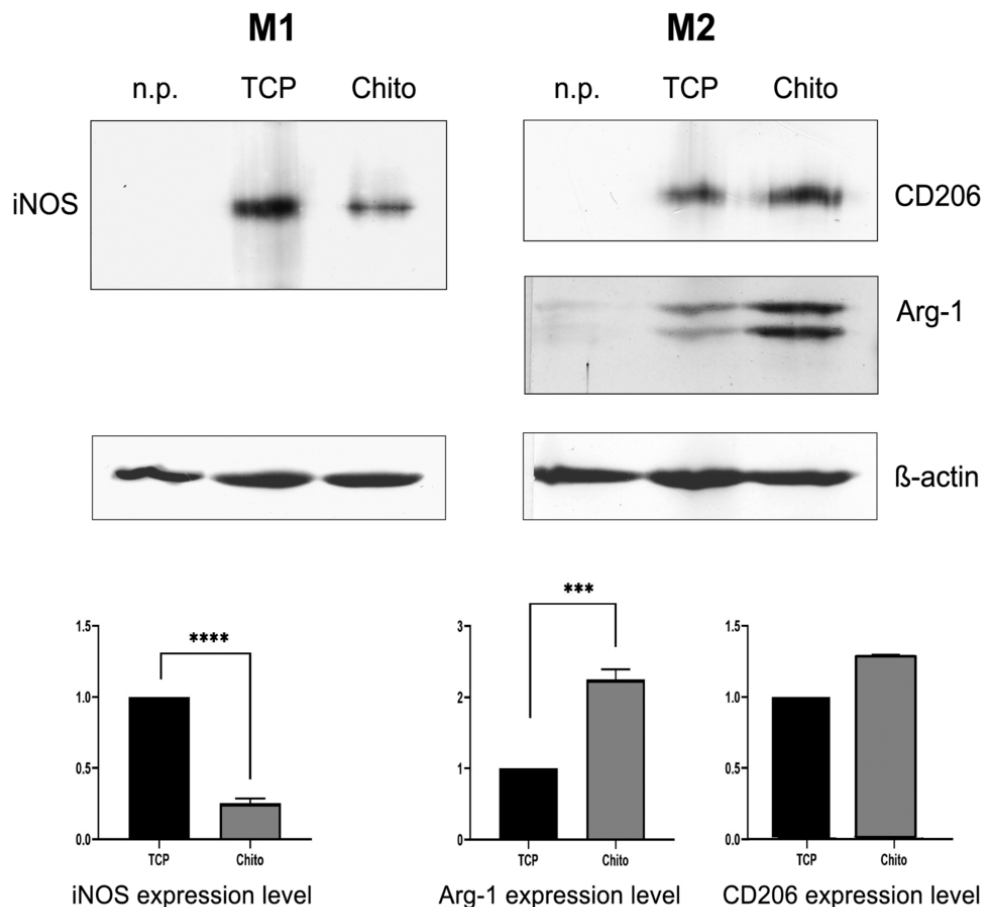


Fig 2: Impact of chitosan-FPHS substrate (2% DA, 2.5% Cp) on M $\Phi$  polarization in vitro. Compared to M $\Phi$  growing on tissue culture plastic (TCP), on chitosan-FPHS substrate inflammatory M1 marker protein expression (iNOS) is reduced, whereas that of anti-inflammatory M2 marker proteins (Arginase-1, CD206) is enhanced (expression on TCP is set arbitrarily to "1"). M $\Phi$  had been pre-polarized by IFN-gamma/LPS, or IL-4, respectively.  $\beta$ -actin expression is used for reference. Marker protein antibodies are specific, since they do not react with protein extracts from non-polarized (n.p.), "naive" monocytes ("M0"). Note that Arg-1 and actin bands were always revealed simultaneously on the same membrane, the actin band (43 kDa) being situated above that of Arg-1 (35 kDa); the apparent molecular weight of iNOS is ~130 kDa, that of CD206 ~175 kDa. n=4, \*\*\* p=0,0001, \*\*\*\*p<0,0001 (Student's t-test).

83x79mm (300 x 300 DPI)

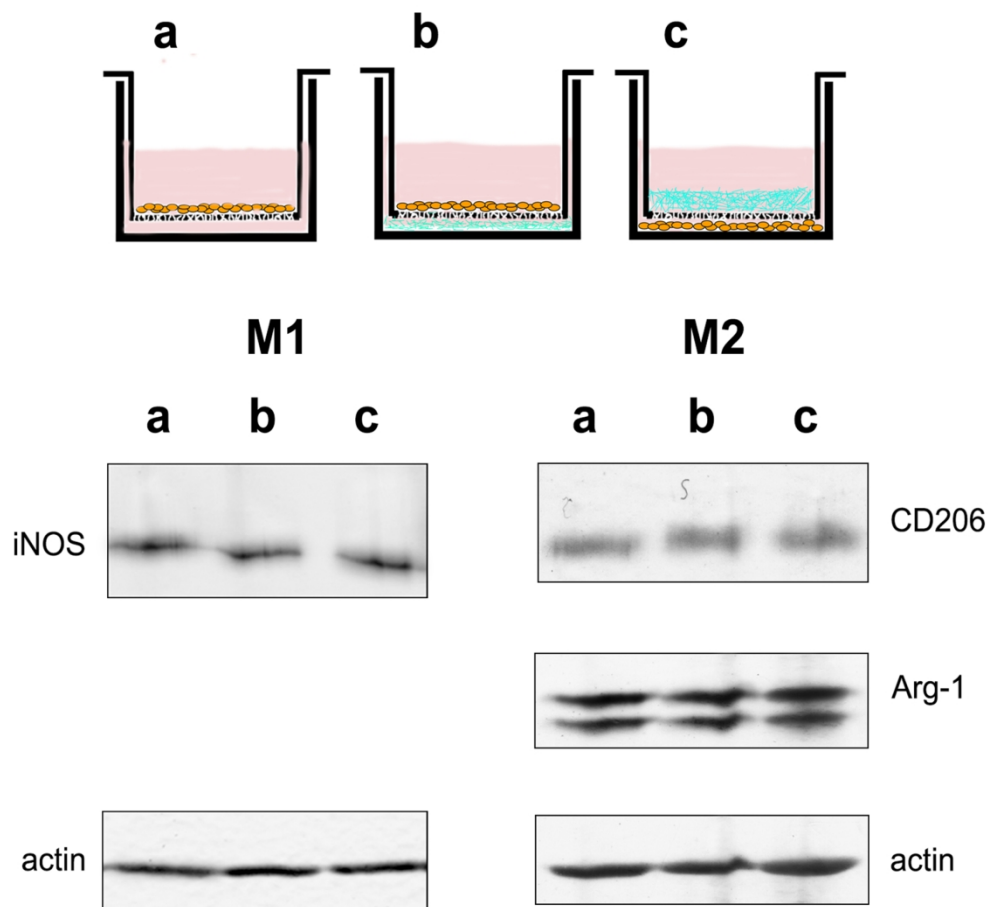
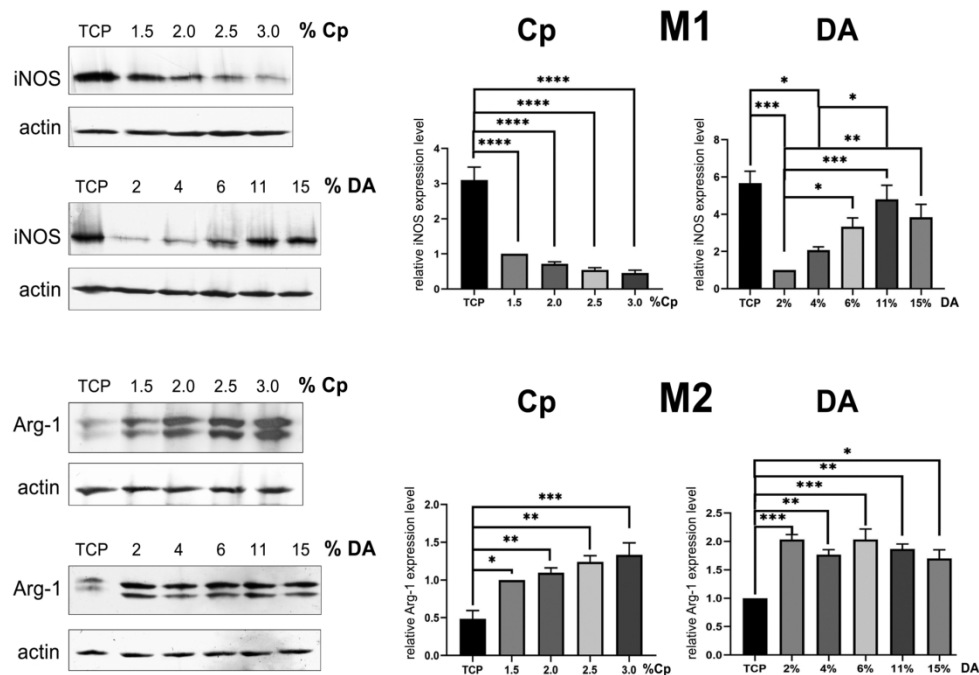


Fig 3: Polarizing effect of chitosan-FPHS depends on direct contact with M $\Phi$ . In insert cultures (3.0  $\mu$ m pores), in which M $\Phi$  are not in direct contact with chitosan-FPHS substrate, the latter has no influence on M1 or M2 M $\Phi$  marker protein expression. The sketch shows the different culture types in cross-section: (a) M $\Phi$  (orange) grow on the insert membrane (red: culture medium), no chitosan present; (b) a chitosan particle film (green) is generated on the bottom of the well, and M $\Phi$  seeded within the insert are separated from the chitosan layer by the porous membrane; (c) M $\Phi$  are seeded on the bottom of the well and a dense chitosan-FPHS slurry is added into the insert.



**Fig 4:** Influence of chitosan concentration (Cp) and DA of the hydrogel particle substrate on MΦ polarization. For statistical evaluation the values obtained for one specific condition were arbitrarily set to 1. M1 MΦ (top): There is a tendency of decreasing iNOS levels with increasing Cp (n=4), while in contrast, increasing the DA leads to significantly increasing iNOS expression that almost reaches control (TCP) values for 11% and 15% DA (n=5). M2 MΦ (bottom): M2 marker protein expression exhibits a tendency to increase with increasing Cp (n=4), while being very little, if at all affected by changes in DA (n=3). Higher DA chitosans (6%, 11%, 15%) were prepared by reacetylation of 2% DA chitosan. Note that the observed impact of chitosan-FPHS on MΦ polarization may not be extrapolated to much higher Cp or DA values. One-way ANOVA with Tukey's post-hoc test, \* p<0.05, \*\* p<0.01, \*\*\* p<0.001, \*\*\*\* p<0.0001 (see also Figs. S1, S2, and Table S1).

180x125mm (300 x 300 DPI)

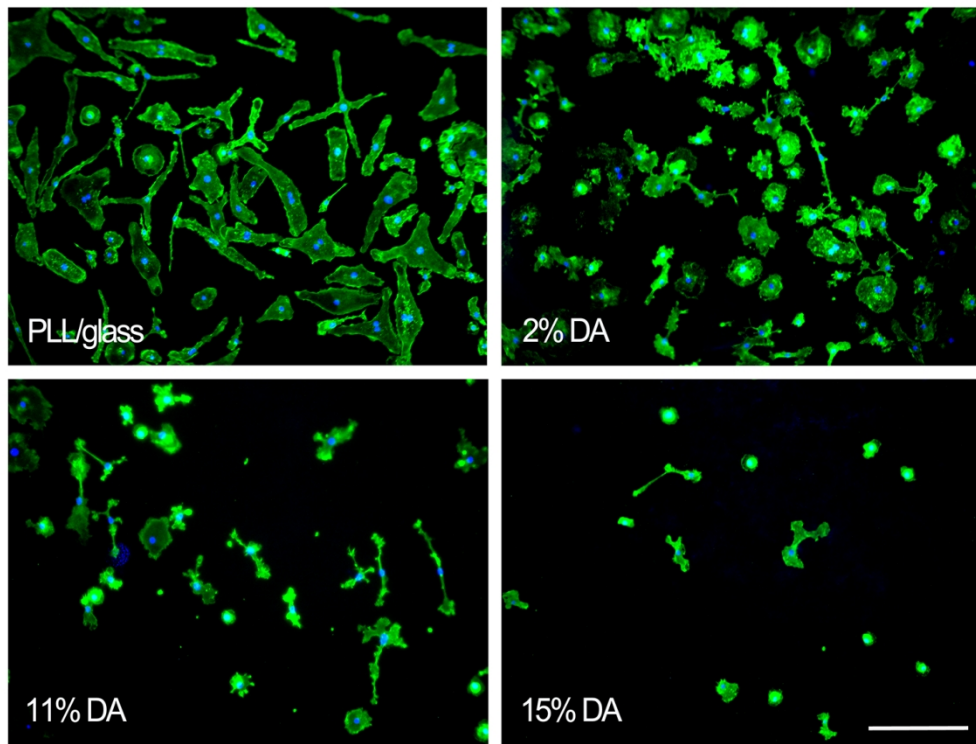


Fig 5: Transwell cultures of M2 M $\Phi$ . Migration of M2 M $\Phi$  through ThinCert membranes (8.0  $\mu$ m pores) after 4 days of culture, onto control coverslips (PLL/glass), or on chitosan-FPHS layers made of 2%, 11% or 15% DA chitosan (M1 M $\Phi$  did not migrate through the membrane). Note the differences in cell shape between M $\Phi$  having migrated onto PLL/glass vs. a substrate made of 2% DA chitosan-FPHS, and the decreasing numbers and changing morphologies of M2 M $\Phi$  migrating on chitosan-FPHS with higher DA values. Scale bar: 100 $\mu$ m.

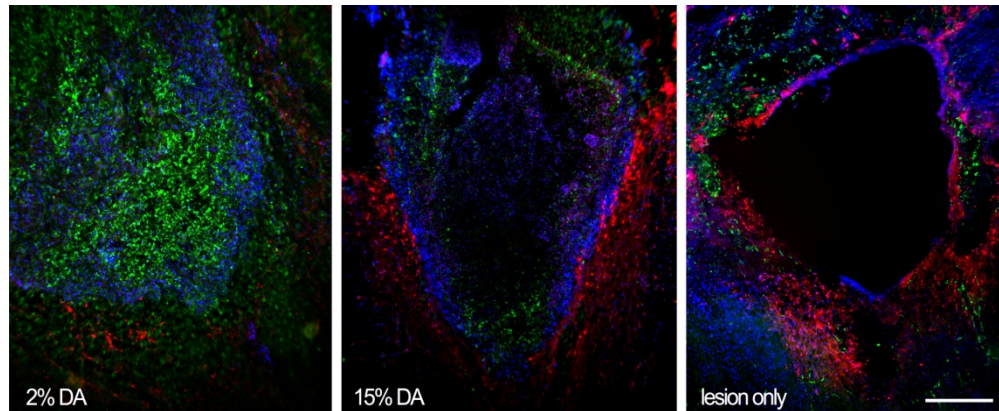


Fig.6: M $\Phi$  phenotype invading chitosan-FPHS in vivo depends on its DA. A dorsal bilateral hemisection of adult rat spinal cord (thoracic level T8-T9) was performed, and the lesion site was either filled with a dense slurry of 2% DA, or 15% DA chitosan-FPHS, or left untreated (lesion only). All animals had a locomotor score of "0" on the BBB scale the day following the lesion. Immunohistochemical staining of horizontal sections of the injured region 2 weeks after the lesion shows that 2% DA chitosan-FPHS is exclusively invaded by M2 M $\Phi$  (CD206 labeling, green), a few M1 M $\Phi$  (CD86 labeling, red) are seen surrounding the lesion site in some distance. Inversely, only few M2 M $\Phi$  are present in a 15% DA chitosan-FPHS implant, and higher numbers of M1 M $\Phi$  found close to the lesion border, without entering the implant. Note that the biomaterial-implanted lesion site is colonized by a high number of cells that will ultimately restore a neural tissue (DAPI nuclear staining, particularly dense at the lesion border). Without chitosan-FPHS implantation, a lesion cavity forms due to tissue necrosis (here at 3 weeks post-injury) surrounded by numerous M1, and some M2 M $\Phi$ . Scale bar: 300 $\mu$ m.

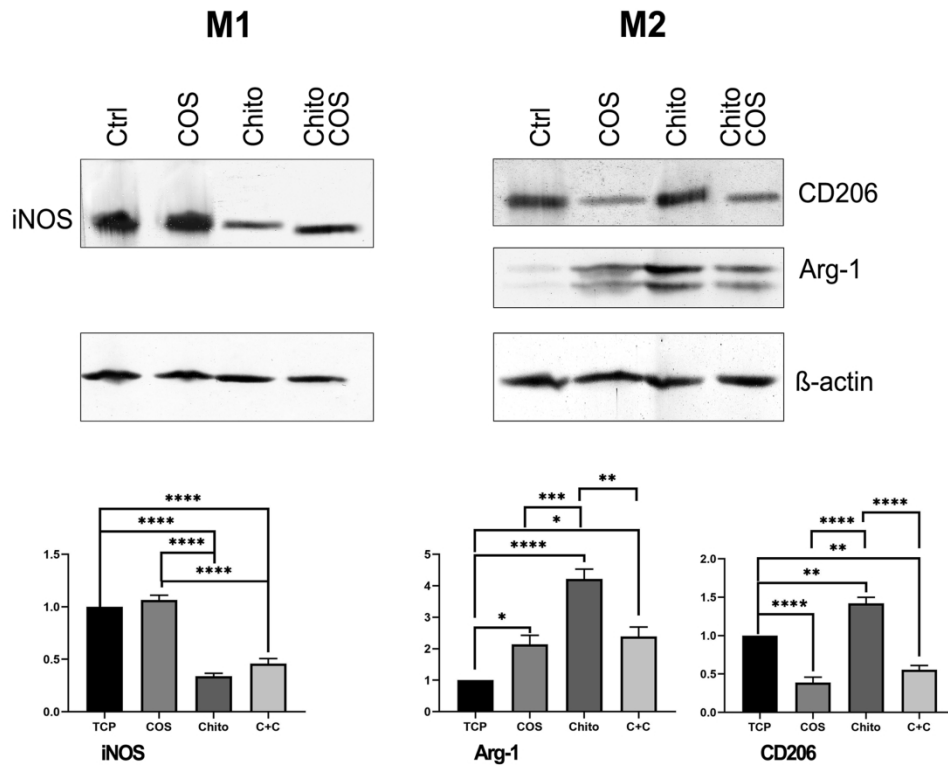


Fig 7: Polarizing effect of chito-oligosaccharides (COS). Addition of a particular type of COS (MW  $\leq$ 1500, DA  $\sim$ 8,5%; 1 mg/mL) to the medium slightly enhances iNOS expression of M1 M $\Phi$  grown on chitosan-FPHS (not significant; n=4). In contrast, in cultures of M2 M $\Phi$  CD206 expression is significantly reduced by the addition of COS on both TCP (Ctrl), and on chitosan substrate (n=4). Presence of COS significantly enhances arginase-1 expression on TCP, but clearly reduces arginase-1 levels on chitosan substrate. TCP (Ctrl): tissue culture plastic; COS: COS addition to culture on TCP; Chito: culture on chitosan-FPHS; Chito/COS (C+C): COS addition to culture on chitosan-FPHS. ANOVA with Tukey's post-hoc test; \* p<0.05, \*\* p<0.01, \*\*\* p<0.001, \*\*\*\* p<0.0001; see also Table S2.

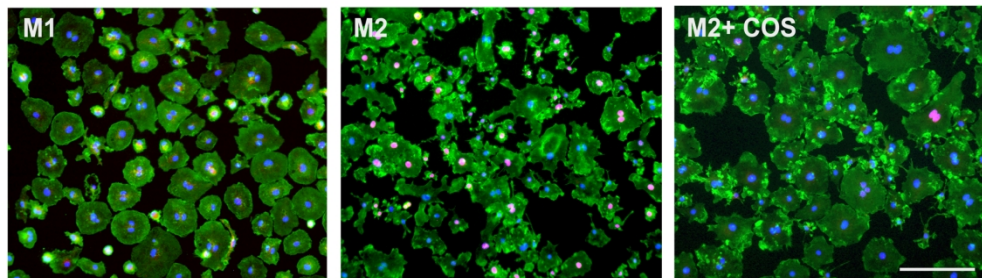


Fig 8: COS treatment alters M $\Phi$  morphology and proliferation rate. M $\Phi$  cultures grown on PLL-treated glass coverslips, stained with proliferation marker Ki67 antibody (red), phalloidin (F-actin, green), and DAPI (nuclei, blue). M1 M $\Phi$  show a rounded morphology, and weak proliferation. In comparison, M2 M $\Phi$  exhibit a much stronger mitotic activity, which is greatly reduced upon addition of COS. Also note the change in morphology between COS-treated and -untreated M2 M $\Phi$ . Scale bar: 100 $\mu$ m.

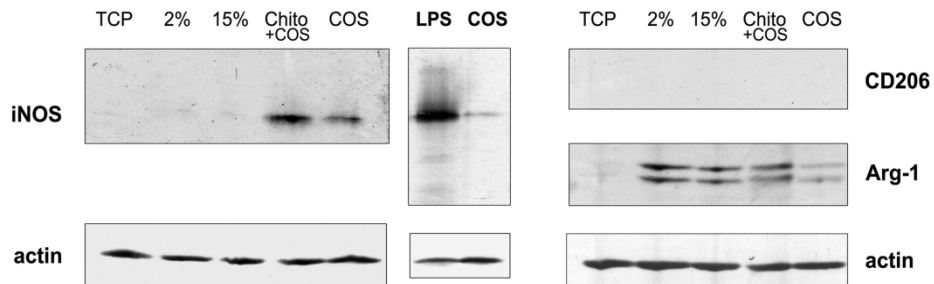


Fig 9: Impact of chitosan-FPHS substrate and COS on non-polarized monocytes. Neither 2% nor 15% DA chitosan-FPHS substrate induce expression of M1 marker protein iNOS by naïve monocytes, but a faint iNOS expression is observed after addition of COS to the culture medium (1mg/mL), even slightly enhanced in the presence of 15% DA chitosan-FPHS. However, the absolute levels of iNOS expression by naïve monocytes induced by COS addition are in fact very low, and cannot be directly compared with those observed in LPS-induced M1 M $\Phi$  (middle panel: the revelation reaction was allowed to continue until appearance of a faint iNOS band from the COS-only polarized sample). In contrast, chitosan-FPHS (both 2% and 15% DA) culture substrates are seen to elicit some low level arginase-1 (but not CD206) expression from naïve monocytes that is slightly diminished by addition of COS. TCP: tissue culture plastic; Chito+COS: 15% DA chitosan plus COS addition.

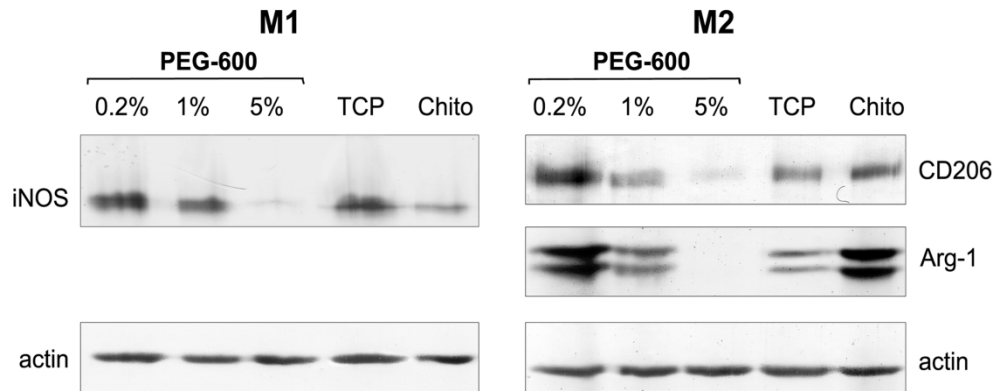


Fig 10: PEG-600 has no specific impact on M $\Phi$  polarization in culture. While low concentrations of PEG (0.2%) in the medium appear to enhance marker protein expression at least for M2, and probably also M1 M $\Phi$  (iNOS levels being comparable to those obtained on TCP, Arg-1 levels to those on chitosan-FPHS substrate), higher concentrations then gradually provoke a reduction in both M1, and M2 marker protein expression.